Investigation of Transient Response of an Unbalanced Aero-Engine Rotor with Semi-Active Damper System

M. Rajasekhar[1] and Dr. J. Srinivas[2]

[1]*Gitam Institute of Technology, Visakhapatnam 530045*
[2]*NIT- Rourkela, Rourkela, Orissa.*

Abstract

This paper deals with dynamics and control of low pressure (LP) turbo-compressor rotor of aero-engines using electromagnetic damper system. Electro dynamically stabilized levitation for high speed rotors are essential in several rotor bearings system. The relative motion between conductor and magnetic field induces eddy currents inside the conductor, there by generating magnetic forces which are used to achieve levitation. The rotor dynamic analysis of an integral shaft over a flexible ball-bearing supports is conducted initially using finite element model. The model considers the ball-bearing contact forces, unbalance forces in compressor and turbine disks as well as gyroscopic and viscous damping terms. After predicting the critical speeds of the rotor, the design of magnetic damper begins. The parameters of the electromagnetic dampers are predicted within the operating speed range, so as to suppress the vibration amplitude at resonance conditions. Results of unbalance response are presented to illustrate the effectiveness of the controller.

1. Introduction

Reduction of vibrations of aero engines is an important application in rotor dynamics. In addition to the safety requirement of avoiding rotor bend critical speeds within the engine running range, the response of the many other modes of the rotors and engine structural system must be controlled to ensure acceptable levels of vibration. Control of vibration is essential in respect of the bearing loads, structural fatigue loads, rotor/casing tip clearances, casing and engine external responses, and transmission of vibration to the airframe. Ewins [1] presented an overview of vibration problems which are experienced in running gas-turbines and other high speed machinery using hydrodynamic bearings. The main disadvantages of these bearings are their passive nature, instability and very sensitive variability of performance with raise in temperatures and frequencies of the rotors.

Rotor damping at the bearings is mostly needed near critical speeds and is relatively ineffective at other speeds. Sufficiently strong electric or magnetic field have been employed in hydrodynamic bearings [2]. Vance et al. [3] reported the application of such actively controlled dampers for aero-engine rotors. Cavalini et al.[4] presented a semi-active vibration control approach dedicated to rotating machine passing by its critical speed during the transient rotation by means of a smart spring mechanism.

Tonoli et al. [5] suggested recently passive or semi-active eddy current dampers as an interesting alternative in the near future due to their relative simplicity, improved reliability and lower cost compared with active devices. Kligerman et al. [6, 7] reported the application of eddy-current dampers to rotor dynamic systems.

Tonoli [8] mentioned the promising application of the transformer/reluctance eddy current dampers, In another article, Tonoli et al. [9] illustrated electromagnetic dampers of active and semi-active type in rotating machines in order to minimize the vibration amplitudes at critical speeds. Here, it is shown the design principles of electromagnetic damper operating over the critical speed range. Athanasios and Dohnal [16] simulated the rotor-bearing system by using a new method for simulation of a multi-segment continuous rotor in combination with nonlinear bearing forces.

The main objective of this paper is to identify the critical speeds of idealized low-pressure rotor in aero-engines and design a damper mechanism that becomes effective within the critical speed regions. The analysis of integral shaft is conducted with the ball bearing contact dynamic force model. Finite element model with Timoshenko beam elements is employed during analysis.

2. Mathematical Formulation

There are different models of aero-engine rotors available in literature. Most common is a twin-spool rotor carrying a central low pressure solid shaft laid concentrically inside a hollow high-pressure (HP) shaft. Analysis of such rotor was studies as case studies earlier [10-12]. In the

present work, the rotor and its supports are representative of the lateral dynamics of the low pressure shaft of an aircraft engine. The low pressure turbine (LPT) and low pressure compressor (LPC) are modeled using two rigid disks connected by a small diameter hollow shaft that is supported by two ball-bearings on the turbine and compressor side. Both the supports are connected to the casing by a set of bars undergoing bending vibration. This model is selected from Holmes and Sykes [13]. When symmetry exists lumping of disk masses is not that much difficult. In order to avoid inaccuracies of such a lumped parameter models, finite element modeling is a convenient way and can be easily programmable. Two-node Timoshenko beam elements are employed to discretize the entire rotor shaft and disks are assumed to be rigid masses. Total four degrees of freedom are included at each node of the rotor model. The ball bearing contact forces Fxi and Fyi (i=1, 2) in x and y directions are applied at the respective bearing nodes 3 and 5 as shown in the Fig.1. At both support nodes 3 and 5, an equivalent stiffness is provided in the model so as to account the effect of flexibility of engine casing.

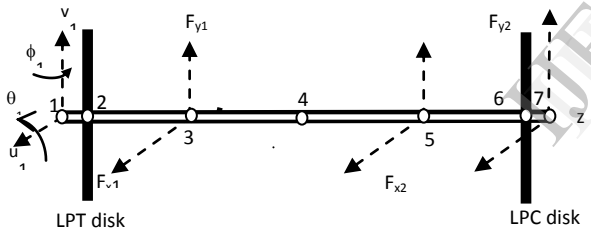

Fig.1 Finite element model of the rotor

The equations of motion for the overall system are written as [14]

$$\mathbf{M\ddot{q}} + \mathbf{C\dot{q}} - \Omega\mathbf{G\dot{q}} + \mathbf{Kq} = \mathbf{f} \qquad (1)$$

where M, C, G and K are respectively assembled mass (includes the shaft mass and disk masses and inertia), damping, gyroscopic and stiffness matrices and q=[q_1 q_2]T, where q_1 is translational degree of freedom, q_2 is rotational degree of freedom of the element assembly. The rotor speed Ω defines the radial unbalance forces and ball bearing contact forces on both the disks. The force vector {F} comprises of the unbalance and contact forces at the respective nodes. The unbalance force components $m_i e\Omega^2 \cos \Omega t$ and $m_i e\ \Omega^2 \sin\Omega t$ (i=1, 2) at the turbine and compressor disks are included at corresponding nodal degrees of freedom of the assembly. The contact forces at the ball-bearings are obtained from Hertzian contact stress-theory. The components of this force are summation of the forces at each ball [15] and are given as:

$$Fx_i\,(i=1,2) = -\sum_{j=1}^{N} C_b(\delta_j)^{1.5} \cos\theta_j \qquad (2)$$

$$Fy_i\,(i=1,2) = -\sum_{j=1}^{N} C_b(\delta_j)^{1.5} \sin\theta_j \qquad (3)$$

Here, N is number of balls, C_b is contact stiffness, θ_j the angular position of j^{th} ball is a function of time (t) and radii of inner, outer races and balls (r, R, r_b), defined by

$$\theta_j = \frac{2\pi}{N}(j-1) + \frac{\Omega rt}{(R+r)} \qquad (4)$$

Also, θ_j is the radial deformation of j^{th} ball due to inner-race displacements (x, y) exceeding the radial clearance (r_0) limit and is given by:

$$\theta_j = x + (r + 2r_b)\cos\theta_j + y + (r + 2r_b)\sin\theta_j - r_0 \qquad (5)$$

This radial deformation should only be considered when it is positive. The entire system is now giving a nonlinear response due to the parametric nature of the forces.

3. Control of vibrations at critical speeds

In order to minimize the vibration amplitudes at the critical speeds of operation of the rotor, it is proposed to design the electromagnetic dampers, which are to be laid at the two support bearing locations. Basically, these dampers have an electromagnet and a mechanical spring. In absence of electromagnet, it works as a hysteretic damper and damping action occurs with respect to the rotor speed. In a magnetic damper the reluctance of the magnetic circuit is influenced by the speed of the moving part in the circuit. This produces a flux variation and generates a back EMF and ultimately eddy currents in the coils.

There are two effects of this eddy current:
1. Generating a force that increases with decrease in air gap, responsible for a negative stiffness.
2. Generation of damping force acting against the speed of the moving element.

In semi-active type of magnetic damper (SAMD) [7] to be implemented in present work, voltage in the coil is kept constant and no closed loop position feedback is necessary as only current in the coil is monitored. Energy dissipation takes place in the stator. We can define the transfer function between the speed of rotor and electromagnetic force (F_{EM}) in terms of pole frequency ω_{RL} as:

$$\frac{F_{EM}}{\dot{q}} = \frac{k_{EM}}{s(1+\frac{s}{\omega_{RL}})} \quad (6)$$

where $k_{EM} = -\frac{2V^2}{RG^2\omega_{RL}}$ is negative stiffness coefficient and pole frequency $\omega_{RL}=R/L_0$;

here $L_0 = \frac{\mu_0 N^2 A}{2G}$ is inductance of each electromagnet at nominal air gap G, 's' is Laplace variable, is speed of the moving part of magnetic circuit. R is total resistance (coil resistance and additional resistance to tune the electric circuit pole). Also N is number of turns of each winding, A is area of magnetic circuit at the air gap and μ_0 is magnetic permeability of vacuum.

In semi-active magnetic damper a mechanical spring of stiffness k_m (where k_m is greater than $-k_{EM}$) is added in parallel to the electromagnet, driven by constant voltage. A better insight can be obtained by studying the mechanical impedance of the damper in parallel to the spring. i.e., for SAMD transfer function will become [7]

$$\frac{F_{EM}}{\dot{q}} = \frac{1}{s}\left[\frac{k_{EM}}{(1+\frac{s}{\omega_{RL}})} + k_m\right] = \frac{k_{eq}}{s}\left[\frac{1+\frac{s}{\omega_z}}{1+\frac{s}{\omega_{RL}}}\right] \quad (7)$$

where $k_{eq}=k_m+k_{EM}$ and $\omega_Z = \omega_{RL}(k_{eq}/k_m)$. It is possible to identify following three different frequency ranges:

1) Equivalent stiffness range ($\omega << \omega_Z$), where the system acts as a spring of stiffness k_{eq}

2) Damping range ($\omega_Z < \omega < \omega_{RL}$), where system behaves as a viscous damper with $c=k_m / \omega_{RL}$.

3) Mechanical stiffness range ($\omega >> \omega_{RL}$), where system acts as a mechanical spring of stiffness k_m.

Fig. 2 shows the mechanical equivalent diagram of SAMD as described in [9].

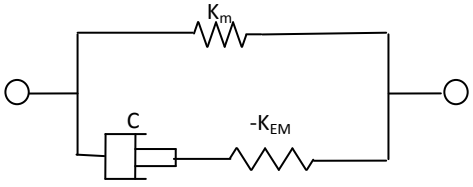

Fig.2 Mechanical Equivalent of eddy-current transformer damper

A sort of constant gain-bandwidth product characterizes the damping range of the electromechanical damper. This product $k_m = c\omega_{RL}$ is just a function of the spring stiffness included in the damper. The constant gain-bandwidth means that for a given electromagnet, an increment of the added resistance leads to a higher pole frequency but reduces the damping coefficient of the same amount.

3.1. Specifications

The knowledge of the resonant frequencies at which the dampers should be effective and the maximum acceptable response allows in specifying the needed value of the damping coefficient (c). The pole and zero frequencies (ω_{RL}, ω_Z) have to be decided so that the relevant resonant frequencies fall within the damping range of the damper. Additionally, tolerance and construction technology considerations impose the nominal air gap G. Electrical power supply considerations lead to the selection of the excitation voltage V.

3.2. Definition of the SAMD parameters

The mechanical stiffness can be obtained as $k_m=c\omega_{RL}$, once the pole frequency (ω_{RL}) and the damping coefficient (c) are given by the specifications. The electromechanical parameters of the damper viz., the electromechanical constant N^2A and the total resistance R can be determined as follows:

a. The required electrical power V^2/R is obtained from $V^2/R=0.5G^2\omega_{RL}\ k_m\ (1-\omega_z/\omega_{RL})$. The knowledge of the available voltage V allows then to determine the resistance R.

b. The electromechanical constant N_2A is then found using $L_0=R/\omega_{RL} = \frac{\mu_0 N^2 A}{2G}$

4. Results and Discussion

The entire finite element analysis process starting from generation of nodal connectivity and element matrices, assembly together with static condensation for elimination of rotational degrees of freedom and posing boundary conditions is performed by an interactive computer program written in MATLAB. Further, the Campbell diagram for the rotor illustrating variation of its natural frequencies as a function of speed Ω and time-domain characteristics using Wilson-theta implicit time-integration scheme (with step

size=1e-4 s) are obtained for the reduced-order system before and after implementing the proposed electromagnetic damper. Main parameters of rotor considered include:

Rotor Shaft:

Outer diameter =25 mm, Inner diameter =15 mm, Material (alloy steel): Elastic modulus E=207 GPa, density (ρ) =7840 kg/m^3, Poisson ratio μ=0.3, eccentricity of center of masses (e)=10 microns, shear correction factor k=0.65.

Ball bearings for LPT and LPC sides:

Number of ball N=8, radial clearance r_0=20 microns, inner race radius r=20.046 mm, outer race radius R=31.95 mm, contact stiffness at balls C_b=3.527×10^9 N/m$^{3/2}$, ball radius r_b=(R-r-r_0)/2=5.94 mm, Stiffness at both rotor supports on casing=300 kN/m.
Other geometrical data of rotor rig (see Fig.1) is depicted in Table 1.

Table.1.Data for the rotor dynamic rig under consideration (+ bearing nodes)

Node Number	Axial distance (mm)	Disk dimensions (mm)	
		Diameter	Thickness
1	0	--	--
2(LPT disk)	20	150	10
3+	75	--	--
4	200	--	--
5+	325	--	--
6(LPC disk)	380	150	10
7	400	--	--

Fig.3 shows the Campbell diagram of the rotor supported on the casing.

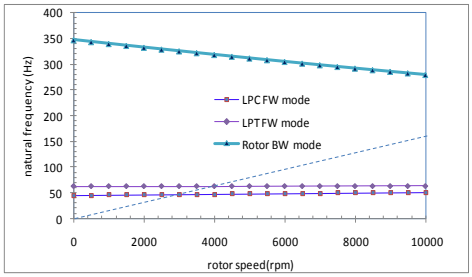

Fig.3 Campbell Diagram for supported rotor

As can be seen, the first two critical speeds (about 2684 rpm and 3767 rpm) are in the operating range, while the third is far above. Fig.4 shows the unbalance response of rotor at the LPT and LPC disks in x and y directions respectively. Fig.5 shows the corresponding frequency response curve at the LPT disk in the zone under consideration.

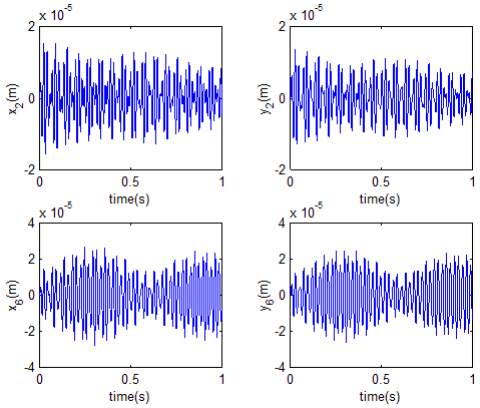

Fig.4 Time histories at turbine (suffix 2) and compressor disks (suffix 6) under 2680 rpm

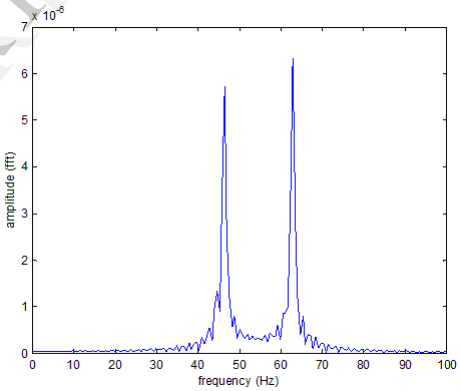

Fig.5 Frequency spectrum before application of actuators

Zero frequency $\omega_z=\omega_{RL}\left(1-\frac{2V^2}{R\omega_{RL}G^2k_m}\right)$

=258rad/s (~2463 rpm)

Electromagnetic Damper Design. During the design of actuators, the following parameters are taken as inputs:
Resonant frequencies at which the dampers should be effective=2500 rpm to 4000 rpm,
Supporting stiffness k_s=300 kN/m

LPC support Damper

Total resistance R=1.1 ohms, Air gap G=0.5 mm, Number of turns N=345, Wire diameter=0.5 mm,

Coil inductance at nominal air gap /electromagnet L_0=2.5 Mh,
$\therefore \omega_{RL}$=electromechanical pole frequency =$1.1\times10^3/2.5$ = 440 rad/s (~ 4201 rpm)
Equivalent damping ratio= 0.0043, Support mass of LPC side m_c=0.287 kg,

Damping coefficient $c_c=0.0043\sqrt{300\times10^3/0.287}$ =4.396 Ns/m.
Mechanical stiffness $k_m=c_c\omega_{RL}$=1934.24 N/m, Supply voltage V=0.2 volts

LPT support damper

Total resistance R=1.85 ohms, Air gap G=0.5 mm, Number of turns N=352, Wire diameter=0.5 mm,
Coil inductance at nominal air gap/electromagnet L_0=3.7 mH
$\therefore \omega_{RL}$=electromechanical pole frequency =$1.85\times10^3/2.5$ =500 rad/s (~ 4774 rpm)
Equivalent damping ratio= 0.003, Support mass m_t=0.19 kg,

Damping coefficient $c_t=0.003\sqrt{300\times10^3/0.19}$ =3.7696 Ns/m.
Mechanical stiffness $k_m=c_t\omega_{RL}$=1884.84 N/m
Supply voltage V=0.242 volts

Zero frequency $\omega_z=\omega_{RL}\left(1-\frac{2V^2}{R\omega_{RL}G^2K_m}\right)$=365 rad/s (~3485 rpm)

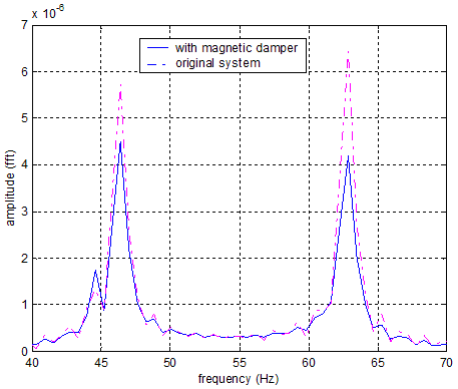

Fig.6 Unbalance response with the actuator system

Activating the two damper systems in respective speed ranges, an unbalance response as shown in Fig.6 is obtained. It is seen that outside the selected region, the amplitudes are not much affected. Fig.7 shows the time-varying damping forces acting on the supports so as to attenuate the vibration amplitudes in first two critical speeds regions. The system is under the action of equivalent spring k_{eq} from 0 to ω_Z rad/s and under the mechanical stiffness k_m in the range beyond ω_{RL}. The spring forces can also be likewise plotted to show their effective ranges.

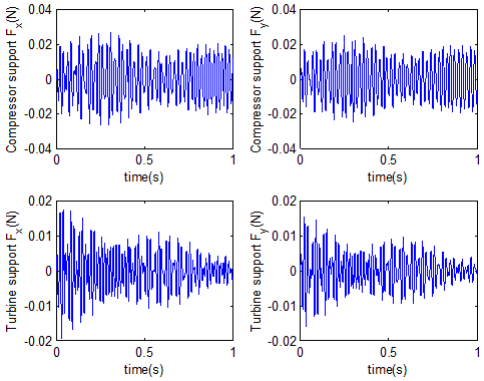

Fig.7 Corresponding damping forces

5. Conclusions

A semi-active technique for vibration attenuation through electromagnetic actuator has been presented in this paper. The system works by changing the structural parameters of an aero-engine rotor supports. Numerical simulations were conducted using finite element analysis of rotor having hollow circular shaft with compressor and turbine disks supported over the engine housing. Critical operating regions were identified with the Campbell diagram and the corresponding time and frequency responses have been plotted to know the regions and amplitudes of interest. Analytical design of actuators for compressor and turbine rotor supports were explained. Attenuation result was illustrated with frequency spectra and corresponding damping force history was also shown. Real time implementation of this semi-active (without sensor) magnetic actuator system is needed to understand more insights in the design.

6. References

[1] D.J.Ewins, "Control of vibration and resonance in aero-engines and rotating machinery-An overview", *International Journal of Pressure Vessels and Piping*, 2010, 87,pp.504-510.
[2] S.Lim, S.M.Park and K.I.Kim, "AI Vibration control of high-speed rotor systems using Electrorheological fluid". *Journal of Sound and Vibration*, 2005, 284, pp. 685- 703.
[3] J.M.Vance, D.Ying and J.L.Nikolajsen, "Actively controlled bearing dampers for aircraft engine applications", *Journal of Engineering for Gas Turbines and Power, Trans. ASME*, 2000, 122/3, pp.466-472.
[4] A.A.Cavalini, T.V.Galavotti, T.S.Morais, E.H.Koroishi and V.Steffen, "Vibration attenuation

in rotating machines using smart spring mechanism", *Mathematical Problems in Engineering* 2011, pp.340235-340248.

[5] A.Tonoli, N.Amati and M.Silvagni, "Transformer Eddy Current Dampers for the Vibration Control", *Journal of Dynamic Systems. Measurement and Control, Trans. ASME*, 2008,130, pp. 031010-031018.

[6] Y.Kligerman and O.Gottlieb, "Dynamics of a rotating system with a nonlinear eddy-current damper", *Journal of Vibration and Acoustics, Trans. ASME*, 1998, 120/4, pp. 848-853.

[7] Y.Kligerman, A.Grushkevich and M.S.Darlow, "Analytical and experimental evaluation of instability in rotor dynamic system with electromagnetic eddy-current damper", *Journal of Vibration and Acoustics, Trans. ASME*, 1998, 120/1, pp. 272-278.

[8] A. Tonoli, "Dynamic characteristics of eddy current dampers and couplers". *Journal of Sound and Vibration*, 2007, 301, pp. 576- 591.

[9] A.Tonoli, N.Amati, A.Bonfitto, M.Silvagni, B.Staples and E.Karpenko, "Design of Electromagnetic Dampers for Aero-Engine Applications", *Journal of Engineering for Gas Turbines and Power, Trans. ASME*, 2010, 13/2, pp.112501-112511.

[10] A.Shanmugam and C.Padmanabhan, "A fixed-free interface component mode synthesis method for rotor dynamic analysis", *Journal of Sound and Vibration* 2006, 297, pp.664- 679.

[11] P.M.Hai and P.Bonello, "An Impulsive Receptance Technique for the time Domain computation of the Vibration of a Whole Aero-Engine Model with nonlinear bearings". *Journal of Sound and Vibration* 2008,318, pp. 592– 605.

[12] P.Bonello and P.M.Hai, "A receptance harmonic balance technique for the computation of the vibration of a whole aero-engine model with nonlinear bearings". *Journal of Sound and Vibration,* ,324, pp. 221– 242.

[13] R.Holmes and J. E. H.Sykes, "The Vibration of an Aero-Engine Rotor Incorporating Two Squeeze-Film Dampers". *Journal of Aerospace Engineering, Proceedings of IMechE, Part G* , 210, p**p**. 39 – 51.

[14] KM.R.Movahhedt and P.Mosaddegh, "Prediction of chatter in high sped milling including gyroscopic effects". *Int. Journal of Machine Tools and Manufacture*, 2006,46. pp. 996 – 1001.

[15] T.C.Gupta, K.Gupta and D.K Sehgal, Instability and chaos of a flexible rotor ball bearing system: An investigation on the influence of rototing imbalance and bearing clearance", *Journal of engineering for Gas turbines and power, Trans of ASME,* 2011,133, pp. 082501-082511.

[16] Anthanasalevris and Fadi Dohnal, "Vibration quenching in a large scale rotor-bearing system using journal bearings with variable geometry" *Journal of Sound and Vibration,* 2014, 333, pp.2087–2099